

The Proof-of-Concept (POC) Model of the REHOS Ejector Heat Pump_Part 1

**by
Johan Enslin**

Heat Recovery Micro Systems

**Heidelberg
South Africa**

Abstract:

As the REHOS Power cycle is really a combination of two sub-cycles, namely a Heat Transformer type heat pump, coupled regeneratively to an Organic Rankine Power cycle (ORC), the various concepts and principles it consist of were looked at and the only concept not yet demonstrated academically (and commercially) is identified for demonstration in a PoC Model.

Some basic definitions and conventions regarding efficiency calculation for Vapor Compression (VC), Absorption Heat Transformer (AHT), as well as AHT-VC Hybrid Heatpumps are discussed, and also compared to the thermodynamic ideal (Carnot and Lorenz) cycles. Although the electric component of efficiency (COP_e) is very high for the AHT-VC Hybrid type Heatpump (like the REHOS Ejector Heatpump), it is shown to be a convention only, and it does not violate any thermodynamic laws.

The current status of the Commercialization of the REHOS Technology is presented, and the choice of the first PoC Model motivated. A detailed design of a proposed Proof-of-Concept (PoC) REHOS Ejector Heatpump including the design of the ejector-type compressor is presented, with the theoretically calculated results of all process parameters included. This paper is part 1 of a two-part series and the part 2 should be detailing the actual experimental values after this PoC Model was built and tested, for comparison to the theory provided in this part 1.

The list inclusive of some 22 references of academic and commercial publications cited, also include 8 publications from the author of this paper, providing more information published on his website.

Introduction:

The Regenerative Heat of Solution (REHOS) thermodynamic cycle basically consist of two sub-cycles, coupled regeneratively. A heat transformer (AHT) type heat pump as primary sub-cycle, provide the pumped (upgraded) heat to an Organic Rankine Cycle (ORC) that produce power from it (power sub-cycle). The heat rejected from the ORC is regeneratively re-used as input, low temperature (degraded) heat by the heat pump, in addition to external waste heat (or ambient heat from the environment) upgraded by the heat pump.

In this combination, the power sub-cycle (ORC) generate power, while the heat pump sub-cycle use power to drive it. The combined REHOS Power cycle power output would be the ORC power generated, minus the Heatpump power used. With a standard Vapor Compression (VC) heat pump as primary sub-cycle, the electrical power used by the compressor would be more than the ORC power that is generated, making the netto power output negative. This is even exaggerated by the non-perfect operation of the sub-cycles. It is therefore very important to carefully choose the type of heat pump for minimum electricity used (and more heat driven) to maximize the REHOS netto output power. Both the sub-cycles used are also subject to the normal thermodynamic physical constrains, and operate at efficiencies of around 60 - 70% Carnot. To stay realistic, we have to assume for further discussions the sub-cycle thermodynamic efficiencies to be 65% of the ideal, which is consistent (conservative) with many published papers on practical ORC and Heatpump machines.

VC heat pumps use electrical energy to drive the compressor, powering the heat upgrading process, while AHT type heat pumps use intermediate temperature external heat for this purpose. The AHT operate on the Osenbrück cycle (replace the VC heat pump cycle condenser and evaporator, with an absorber and desorber), using intermediate temperature heat in the desorber to power the heat upgrading process. A typical example was presented by Rivera [4] using the single stage AHT to upgrade the heat in a Solar Pond to higher temperature. This cycle reduce the pressure ratio (as required by the VC heat pump) substantially for the same heat pumped capacity. The coefficient of performance (COP), defined as the Heat Pumped (Q_{hot}) divided by the Energy Powering this process for the AHT would be for heating service (delivering high temperature heat as (Q_{hot}) using intermediate temperature heat as (Q_{used}) and defining liquid pumping power as (W_{pump}) :

$$COP_{AHT} = \frac{Q_{hot}}{(Q_{used} + W_{pump})}$$

but because the hydraulic pumping energy in general is some two orders of magnitude smaller than the heat component, it is generally ignored in the COP calculation. The COP for the VC heat pump is dependant on the compressor power ($W_{compress}$) and is defined as:

$$COP_{VC} = \frac{Q_{hot}}{W_{compress}}$$

Recently some AHT-VC Hybrid heat transformers have been developed, using both intermediate temperature heat and electric power to drive the heat upgrading process. This was presented by Nordtvedt [2] in 2011, and Borgås [6] in June 2014, and comprehensively analyzed by Jensen [5] in December 2015. The COP for these Hybrid heat pumps can be defined as:

$$COP_{hybrid} = \frac{Q_{hot}}{(Q_{used} + W_{compress})}$$

All heat transformers use the principle of generating high temperature liquid mixtures by forcing vapor to be absorbed into a liquid, transferring both the latent heat of condensation and the Heat of Solution (HOS) to the absorber liquid. In the Hybrid heat transformers, this vapor required is partially produced by heat (Q_{used}), boiling off vapor from a saturated liquid mixture in a desorber, and partially by a compressor ($W_{compress}$) removing and compressing the vapor to the absorber pressure.

HOS type heat pumps also allow sliding temperature heat source and sink, allowing operation on the high efficiency Lorenz cycle. This was extensively elaborated on by Jensen [5]. In this cycle, both the desorber and absorber operate at their own fixed pressures, but sliding temperatures brought about by ammonia concentration changes (in the NH₃ in aqua zeotropic binary mixture). This allow by way of an example, the desorber to operate at fixed pressure, but the local temperature in the desorber following the decreasing temperature of the liquid being cooled. Should hot water at ($T_{intermediate} = 35^{\circ}\text{C}$) be available, it may enter the desorber at the ($T_{desorb_hot} = 30^{\circ}\text{C}$) point and is gradually cooled in the heat exchange coil to 5°C , at the point where the desorber liquid temperature is ($T_{desorb_cold} = 0^{\circ}\text{C}$), allowing heat to be exchanged across this constant 5°C delta, decreasing entropy generation and increasing reversibility when compared to fixed temperature heat exchange. For efficiency calculations the desorber temperature would then be the Log Mean Temperature Delta ($LMTD_{desorb} = 14,74^{\circ}\text{C}$), instead of the single fixed temperature (T_{desorb_cold}) as used in the Carnot cycle. Similarly the absorber may operate at a fixed pressure with high temperature ($T_{absorb_hot} = 60^{\circ}\text{C}$) and the low temperature being ($T_{absorb_cold} = 30^{\circ}\text{C}$) with Log Mean Temp Delta being ($LMTD_{absorb} = 44,76^{\circ}\text{C}$). The ideal Carnot COP of this heat pump for heating service may be written:

$$COP_{carnot} = \frac{(T_{absorb_hot} + 273)}{(T_{absorb_hot} - T_{desorb_cold})} = 5,55$$

while calculation for the ideal Lorenz cycle heat pump, taking into consideration the sliding temperatures in both the desorber and the absorber and using the LMTD to calculate the efficiency, may be written as:

$$COP_{lorenz} = \frac{(LMTD_{absorb} + 273)}{(LMTD_{absorb} - LMTD_{desorb})} = 10,58$$

which is very much higher than the calculated Carnot COP for the same heat pump, but only due to our choice of temperatures used in the calculations. The actual efficiency of the polytropic heat source and sink Lorenz cycle is in fact slightly lower than the isothermal heat source and sink Carnot machine, but the Lorenz calculation is really closer to reality, even though the ideal COP value appears higher due to our convenient way to choose average temperatures for the bulk of the desorber and absorber.

The use of this Lorenz cycle principles was seriously elaborated on in papers handling the development of the Kalina cycle, like Kiesela et al [7] published already in 1996. Other principles of zeotropic binary liquid mixtures are also covered in the thesis of Govindaraju [11] published 2005, while the IEA Handbook on thermally driven heat pumps [3] published in 2013 provide valuable insight into calculation conventions and standards. Calculation of the performance of Heat Transformer Hybrid heat pumps (COP_{hybrid}) would be difficult, as the correct amount of heat used (Q_{used}) is not so easy to obtain. With the assumption we made that the performance would likely be 65% of the ideal (Lorenz) performance, the hybrid performance may however, be calculated:

$$COP_{hybrid} = 65\% \times COP_{lorenz}$$

and with the temperatures generally known, the actual heat used for powering the hybrid heat pump (Q_{used}) may be calculated. This is actually of academic importance only, as in general working with heat pumps using energy in the form of electricity (for powering a compressor), it is most important to know how much electricity is required to power the process. As suggested in the IEA Handbook on thermally driven heat pumps [3], we therefore defined as convenient efficiency measure, an electrical component COP as:

$$COP_e = \frac{Q_{hot}}{W_{compress}}$$

ignoring the heat used (Q_{used}) for the correct (COP_{hybrid}) thermodynamic calculation.

This performance value (COP_e), although not representing the thermodynamically correct performance, is very valuable, as it correctly represents the electrical component of performance using heat transformer hybrid type heat pumps. Care should be taken not to compare the VC type heat pump performance (COP_{VC}), where the compressor power used, reflects the total energy for powering the heat pumping process, with the hybrid (COP_e) where the compressor power is only a part of the energy required for powering the heat pumping process. Comparing VC heat pump performance with heat transformer hybrids should be done by comparing (COP_{VC}) with (COP_{hybrid}), as defined above, only!

Process parameters like temperature, pressure, enthalpy, %NH₃ concentration of ammonia in NH₃ in aqua mixtures etc. mentioned in this document are provided from lookup tables generated in spreadsheets making use of the Thermophysical Properties of NH₃ + H₂O solutions information of Conde-Petit [9] published in 2004, Ganesh and Srinivas [10] published January 2011. Thermodynamic Properties of water and steam is from Keenan et al [12] published 1969 and Saturated and superheated Ammonia by Haar and Galager [13] published in 1978.

Status of the REHOS Commercialization Project:

The IP protection path started with the Provisional Patent Application # 2016/06959 of priority date 11 October 2016, after which various description papers and explanation documents were being released and published. This was followed up with a PCT Application, PCT/IB2017/056283 dated 11 October 2017. The subsequent International Search results from the PCT Examiner was very encouraging, declaring the REHOS cycle and claims New, Inventive and Industrially Applicable, paving the way for full international patenting.

Various papers were written, spelling out the REHOS concept, operation & applications and are available as pdf files downloadable from my website [22]. This include the introduction of the REHOS concepts [15] presented in the PowerGen Africa Conference in July 2017, a paper detailing the Simplified REHOS Cycle [16] in August 2017 where the functions of the absorber and desorber are combined in a single "Bubble Reactor", with another paper to clarify and spell out the process parameters for the Simplified REHOS cycle [17], published October 2017. In addition, the (unpublished) paper detailing the process values and calculation methods around the NH₃-H₂O Bubble Reactor [18] was prepared in December 2017, followed by two papers detailing the competitive advantage [19] in January 2018, and the executive summary of the REHOS technology [20] in February 2018, giving a very brief overview of what REHOS actually mean. This was followed up by a paper written to clarify the high COP values mentioned in previous papers [21] published in March 2018. My latest paper [22] published in April 2018 is an attempt to compare the performance of various heat pumps with each other in extracting low temperature waste heat from the environment for use as heat (space, swimming pool and domestic hot water), refrigeration and air conditioning (de-humidifiers for "Water from Air" extraction) as well as electrical power production (in a benchmark ORC).

The commercialization project involve the demonstration of an initial proof-of-concept (PoC) REHOS Ejector Heatpump model in the next 3 months, followed by power generation pilot plants of various sizes, starting with a small 10 kW_e plant. Demonstrating this Heatpump PoC model is therefore key to unlock the larger finance required for the Commercialization Team to continue with power generation pilots.

Choice of the Proof-of-Concept Model:

The REHOS thermodynamic cycle is a combination of various standard commercially proven principles, with the only concept not commercially proven yet, being the concept of combining the desorber and absorber of an AHT Hybrid heat pump into a single zeotropic binary column. This is the main focus of the project to build and test a proof-of-concept (PoC) model REHOS Ejector Heatpump.

The proposed model is a very low cost and uncomplicated process, in which the bubble reactor (HOS Heat Exchanger) would combine the heat generating absorption process in the bottom of the reactor, while the desorption function would take place in the cold top half of the reactor.

The hybrid heat pump compression function would be performed by a simple vapor ejector type compressor, with no moving parts. These ejector type vapor compressors are ideally suited for very low compression ratio's like this application where only the hydraulic pressure of the liquid column need to be overcome with the compressor. The high pressure vapor to power the ejector compressor is generated by the evaporator heat exchanger coil positioned in the hot bottom of the reactor, where it is heated regeneratively using the low pressure vapor exhausting from the ejector-compressor. This regeneration used with the HOS reactor represent a full REHOS heat pump, where electrical power (W_{pump}) used to drive the liquid pressure pump represent only a small fraction of the heat used (Q_{used}) to power the heat pumping process, as this heat pump is also a true heat transformer.

This proposed REHOS Ejector Heatpump with an electrical performance (COP_e) in the range of 400 - 600 due to the relatively small amount of power used for liquid pumping, would have a huge commercial value in the refrigeration and air conditioning market even as a stand-alone process. Just as an example, standard VC type technology used in dehumidifiers to extract water from air, have been proven commercially to use about 2 MWh_{th} /m³ of water extracted direct from the air, at a cost of about \$58-21 /m³ water, depending obviously on the cost of electricity. (More details were given in my paper [22] on heatpump comparisons.) With this REHOS Ejector Heatpump technology where the largest component of energy used for the heat pumping process is actually waste heat, it would be possible to use as de-humidifier heat pump, using only some 5 kWh_e /m³ water at an electricity cost of ~ \$0-10 /m³ water, less than 1% of current commercial de-humidifiers! This low cost is also less than 5 % of current draught-stricken cities (like Cape Town in South Africa) municipal water bill. (These water cost examples represent operational cost only and does not include capital investment requirements.)

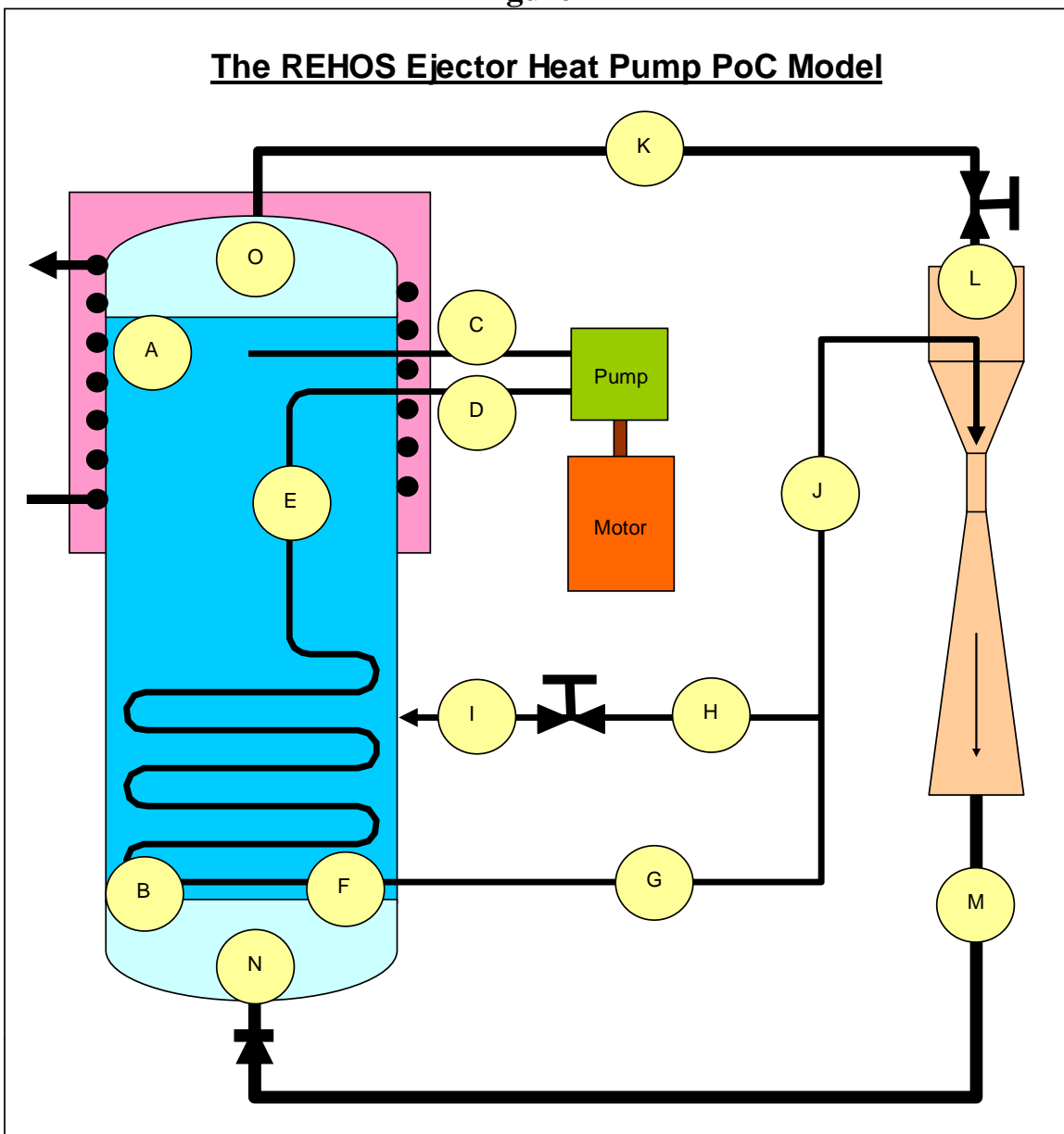
This PoC heat pump model would be a strong first step in the revolution of future power generation using the REHOS Generator, powered by low temperature waste (or ambient) heat from water pools, rivers, lakes and the sea as infinitely huge solar energy reservoirs.

REHOS Ejector Heat Pump Model Design:

The full heat pump process is sketched in figure 1 below. The process lines have been named alphabetically to make reference to it in this description easier. The bubble reactor is colored blue in the figure 1 sketch, where 53%NH₃ is dissolved in water, covering the dark blue section of the reactor, while the light blue sections represent NH₃ vapor in this saturated mixture configuration. Notice the top of the reactor is covered with a heat exchange input heat coil, covered by the pink thermal insulation. This ensure that the amount of heat flowing into the reactor at the cold top can be measured accurately. Pumped heat appearing as higher temperature would be radiating from the un-insulated bottom of the reactor during operation, but is not measured, as it is easily calculated.

The liquid pump used is a Viking gear Pump type SG 40535 RV coupled to a Bircraft

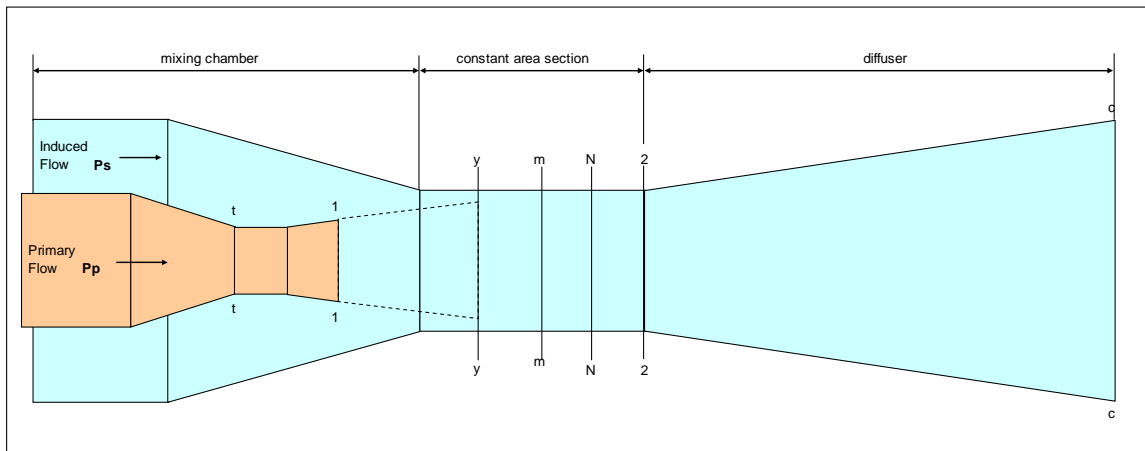
Figure 1



Permanent Magnet 24VDC electrical motor type EC350.240. The pump is coupled to 10mm OD and 8mm ID, SS316 instrumentation tubing, also forming the evaporator coil inside the reactor. The vapor line (K) coupling the reactor top to the ejector inlet is made from 1/2" SS pipe, while the return line from the ejector outlet to the reactor bottom line (M) is a 1" SS pipe, coupling to the bottom of the reactor via a SS non-return valve (NRV). At the reactor bottom a very fine SS wire mesh is positioned as a vapor distributor, to break up the vapor flow in thousands of very small streams to form a multitude of evenly distributed vapor bubbles as it enters the liquid column. During operation this vapor distributor mesh, with the NRV is estimated to generate a backpressure of some 19,3 kPa, while the liquid column hydraulic pressure is only 7,7 kPa in total. In the low pressure vapor line (K) just before the vapor enter the ejector inlet chamber, a SS valve provide a means to slowly start the process. A recirculation liquid line (H) to (I) also has a valve between (H) and (I) for regulating recirculating liquid flow during warm-up.

The ejector compressor was designed according to principles provided in the paper by Chen et al [1] published in April 2013, also corresponding to the naming concepts as used in the paper. The layout is replicated in figure 2 below. Primary inlet vapor flow (P_p) is accelerated to supersonic speed leaving the primary nozzle at position 1-1, creating a low pressure that suck in induced vapor (P_s). The primary supersonic jet flare out and decelerate, increasing the pressure, forming a cone ending at position y-y before mixing with the induced vapor start. The induced vapor flow is compressed by the narrowing space between the inlet chamber outer edge and the supersonic cone, until mixing start at position yy. A normal shock occur at position N-N, decreasing flow speed and increasing pressure prior to the gradual pressurization occurring in the outlet diffuser between position 2-2 and c-c. Four different efficiency estimations is used by Chen, but to be realistic with the use of ammonia in the ejector, we chose estimations some 10 - 20% lower in our design.

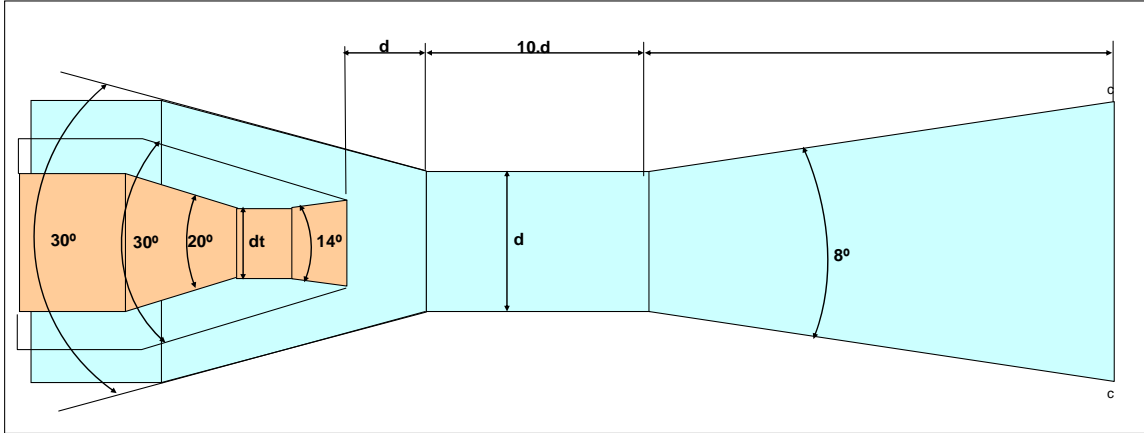
Figure 2



Angles and dimensions are defined as per the sketch in figure 3 below. Actual design dimensions of this model design are listed in table 2 below, with the calculated

operational performance (in an excel spreadsheet) results listed in table 3. The ejector primary nozzle is manufactured from steel, while the tapered inlet, mixing tube and outlet diffuser is manufactured from PTFE. This makes for easy machining.

Figure 3



The rest of the process components as sketched in figure 1, above, are all made from Stainless Steel 316, as the NH3 in aqua mixture is quite corrosive.

Table 1

Model Dimensions

Description	Dimension	Units
Evaporator Coil Tube OD	1.00E-02	m
Evaporator Coil Tube ID	8.00E-03	m
Suction Vapor Tubing 1/2" OD	2.13E-02	m
Suction Vapor Tubing 1/2" ID	1.58E-02	m
Ejector Exhaust Tube 1" OD	3.34E-02	m
Ejector Exhaust Tube 1" ID	2.66E-02	m
Bubble Reactor OD	2.73E-01	m
Bubble Reactor ID	2.65E-01	m
Bubble Reactor Tube Length	0.80E+00	m
Bubble Reactor Cap Height (Outer)	1.52E-01	m

As can be seen from table 2, the ejector is quite small, with the primary nozzle throat diameter (dt) only 1,2 mm diameter, but this was chosen as it was thought that making this throat smaller, would be difficult to retain machining quality.

As shown in the ejector performance table 3, the ejector efficiency at the design point is calculated to be only 44,9% with an entrainment ratio of 4,3 with 27% of the internal vapor frictional loss occurring in the mixing tube, and 23% in the outlet diffuser. This is

actually very realistic for ejector type compressors, making the design calculation fairly realistic and therefore credible.

Table 2

Ejector Dimensions

Description	Dimension	Units
dt	1.20E-03	m
d_nozzle outlet	1.32E-03	m
d_primary inlet ID	8.00E-03	m
d_primary inlet OD	1.00E-02	m
d	6.00E-03	m
Mixing Tube Length	6.00E-02	m
Diffuser Length	1.36E-01	m
Diffuser Divergent Angle	8.00	Degrees
d_diffuser outlet	2.50E-02	m
d_suction inlet ID	4.00E-02	m
d_suction inlet OD	5.00E-02	m
Suction Taper Inlet Length	6.34E-02	m
Suction Inlet Taper Angle of Contraction	30.00	Degrees
Overall Ejector Length	2.59E-01	m

Table 3

Ejector Performance at Design Point

Description	Calculation	Units	% Total
Diffuser Friction Loss	56.7	Watt	23%
Mixer Friction Loss	67.8	Watt	27%
Primary Nozzle Friction Loss	12.4	Watt	5%
Inflow Real Compression	111.5	Watt	45%
Total Heat Used for Compression	248.5	Watt	
Ejector Compressor Efficiency	44.9%		
Ejector Compressor Entrainment Ratio	4.30		
Compressor Pressure Ratio	1.140		

The reactor is filled with 21,7 kg of ammonia and water mixture, with the %NH₃ by mass is 53%. This will give a saturation pressure of 3,64 Bar Abs at the 25°C ambient temperature. These values, together with other process values, are all listed in table 8 below. A lot more process values at each identified labeled point of the process sketched in figure 1 is listed at the design point as tables 4, 5, 6 and 7 attached to this paper as Appendix A.

The physical constraints on the process involve the reactor to be positioned vertical upright with the external tube-coil and thermal insulation at the top. The ejector should be positioned so the complete ejector is physically above the reactor, so that even with the pump not running, liquid does not fill the ejector, preventing it from starting. This is required to get the heatpump started properly.

Initially, before starting the pump, the complete system is in saturation at ambient temperature (25°C at the saturation pressure of 3,64 Bar Abs.) and the NH₃ concentration is the same (53% in the binary liquid and 99,76% in the vapor area's) in all parts of the process. Only gravitation would separate the liquid mixture from the saturated vapor. Initially, before starting the pump, all external heat input to the reactor top would be stopped, as we need to warm up the reactor tank to create the temperature and concentration gradients first. As the binary liquid mixture in the reactor is at saturation point with the reactor top thermally insulated, any heat entering the reactor bottom would slightly increase the temperature and boil off some NH₃ vapor inside the reactor, and the bubbles would rise inside the reactor column to the top. This NH₃ bubble upflow in the reactor create a NH₃ concentration gradient with the NH₃ concentration increasing from the bottom to the top of the reactor. This is accompanied with a temperature gradient with the reactor bottom at a higher temperature than the top, but may initially be only a degree or two. This will not dissipate internally in the reactor, as convection currents are inhibited in the binary mixture. The hotter, lower NH₃ concentration liquid density is higher than the colder, higher NH₃ concentration. Only external radiation to the environment would be removing heat from the reactor bottom and would cause the gradients to dissipate slowly.

With even a very small temperature gradient established, the pump may be started, but with the recirculation start-up valve between (H) and (I) open. The pump would pressurize the (initially very little) vapor present in the HP vapor line (J), initiating the vapor ejector. At this initial stage, the recirc valve must be open, as the pumped liquid contain ~ 53% NH₃ and the balance is water. The amount of vapor boiled of in the evaporator would be small initially, increasing gradually as more and more heat is generated by the absorption of the ejected vapor entering the reactor at (N). This vapor would be absorbed at (B), transferring heat energy to the evaporator at (F) while gradually increasing the NH₃ concentration at (A). Flashing vapor at (A) being extracted by the ejector would also cool the top of the reactor, gradually increasing the concentration and temperature gradients. The recirc start-up valve may also be gradually closed and when design point temperatures of the reactor are approached, the external waste heat source (by low temperature water flow) may be initiated. Final design point process variables are listed in tables attached as Appendix A.

Nomenclature:

M_A = Mass flow in kg/s at position A. (Subscript reflect position, A, B, C etc.)

P_A = Pressure in Pa Abs at position A.

T_A = Temperature in °Celsius at position A.

ρ_A = Media density in kg / m^3 at position A.

H_A = Enthalpy in J/kg at position A. (Enthalpy of all lookup tables (H_2O and NH_3) have been adjusted for liquid at 0°C to have an enthalpy of zero J/kg.)

H_{vE} = Vapor enthalpy of the solution at position E.

H_{lE} = Liquid enthalpy of the solution at position E.

x = Quality of the 2phase mixture arriving at point A as a result of heat (Q_{desorb}) added to the reactor in cooling the mass (N) down from (T_B) to (T_A). This exclude the additional heat added to the reactor top from external sources (Q_{cold}).

$\%NH3_A$ = Concentration ammonia in media at position A.

Q_{evap} = Heat Energy for liquid heating and evaporation of pumped liquid at position F in Watt.

Q_{desorb} = Heat Energy released (negative) when the mass vapor at N, after absorption, gets cooled while flowing upwards in the reactor to point A, in Watt.

$Q_{condens}$ = Heat Energy released when the vapor mass at N is absorbed in the liquid at B, in Watt.

Q_{hot} = Heat Energy delivered to the hot reactor bottom for radiating out to the environment (or used by a heat powered piece of equipment), in Watt.

Q_{cold} = Heat Energy extracted from the external waste heat source (ambient water being chilled) at the reactor cold top, in Watt.

Some of the most important formulas used when calculation of heat balance around the Heatpump cycle:

$$x = \frac{(H_{IB} - H_{IA})}{(H_{vO} - H_{IA})}$$

$$Q_{cold} = (M_O - M_N \times x) \times (H_{vO} - H_{IA})$$

$$Q_{evap} = M_F \times (H_{vF} - H_{lE})$$

$$Q_{desorb} = M_N \times (H_{lA} - H_{lB})$$

$$Q_{condens} = M_N \times (H_{vN} - H_{lB})$$

$$Q_{hot} = Q_{cold} + M_N \times H_N - M_O \times H_O - M_C \times H_C - Q_{evap}$$

Even though the gear pump efficiency is specifically chosen to be very low (only 20% as can be seen in the data presented in table 8, the pump power used is very small (only 4,11 Watt) and therefore the value of (COP_e) is nearly a thousand. The calculated value of (Q_{used}) being so high (2987 Watt) giving us the real COP value of 1,37 calculated from:

$$COP_{Heatpump} = \frac{Q_{cold}}{(Q_{used} + W_{pump})}$$

At the design point, this model REHOS Ejector Heatpump should be able to generate some 4099 Watt of chilling power (Q_{cold}) by using only ~ 4 Watt of electrical energy. The balance of energy required to power the Heatpump comes from a portion of the waste heat ($Q_{used} = 2987$ Watt).

Table 8**Process Parameters at Design Point**

Conventional VC Carnot COP = $[T_c / (T_h - T_c)]$	2.11	
Assumed % Carnot	65%	
Correct Thermodynamic Cold Extract COP_real	1.37	
Heat Used for Heat Transformer (Q_used)	2987	Watt_th
Cooling Service COP_e	997	
Regenerated Evaporation Heat Extracted Q_evap	1731	Watt
Environmental Input Heat Q_cold	4099	Watt
Heatpump Output Heat Q_hot	3850	Watt
Desorption Heat from NH3 flow in Reactor Q_desorb	-3156	Watt
Vapor Bubble Heat Added to Reactor Bottom Q_condens	5582	Watt
W_pump	4.11	Watt_e
Pump Assumed Efficiency	20%	
Pump Compression Ratio	3.23	
Ambient Temperature	25	Celsius
Evaporator H/E Temp Delta	90	Celsius
Environmental Input H/E Temp Delta	45	Celsius
Average Reactor Contents Density	395	kg/m3
Reactor Contents Mass	21.7	kg
Average %NH3 in Binary Mixture	53.0%	
Saturation Pressure of Binary Mix @ ambient conditions	3.64E+05	Pa Abs
Mass Water in Mixture	10.21	kg
Mass NH3 in Mixture	11.51	kg
Total Reactor Liquid/Vapor Mix Volume	5.5017E-02	m3
	55.02	Liter

All the process values are calculated with formulas from the theory, and all attempts have been made to provide realistic results. The true experimental performance, however, should be added for comparison after this proposed PoC REHOS Ejector Heatpump have been constructed and tested. This is planned for part 2 of this paper.

References:

1. A 1D model to predict ejector performance at critical and sub-critical operational regimes, by WeiXiong Chen, Ming Liu, DaoTong Chong, JunJie Yan, Adrienne Blair Little, Yann Bartosiewicz. The paper was published 13 April 2013 in the International Journal of Refrigeration 36 (2013) 1750-1761 and is available online at www.sciencedirect.com.
2. Hybrid Heat Pump for Waste Heat Recovery in Norwegian Food Industry, Stein Rune Nordtvedt, Institute for Energy Technology, Instituttveien 18, N-2027 Kjeller Bjarne R. Horntvedt, Hybrid Energy AS, Ole Deviks vei 4, N-0666 Oslo, Jan Eikefjord, John Johansen, Nortura AS, Rudshøgda, Norway, Stein.Nordtvedt@ife.no. (*This paper was published in the proceedings of the 10th International Heat Pump Conference 2011.*). This paper is also published as part of the IEA Handbook [2], page 57 - 61.
3. Thermally driven heat pumps for heating and cooling, compiled and edited by Annette Kühn (Ed.) as the Universitätsverlag der TU Berlin 2013, as the IEA Handbook available as handbook ISBN (online) 978-3-7983-2596-8 at email publikationen@ub.tu-berlin.de
4. Experimental Evaluation of a single-stage Heat Transformer used to increase Solar Pond's Temperature, by W. Rivera of Centro de Investigación en Energía-UNAM, P.O. Box 34, 62580, Temixco, Mor. , Mexoco and published in Solar Energy Vol 69, No. 5, pp. 369 - 376, 2000.
5. Industrial Heat Pumps for High Temperature Process Applications (*A numerical study of the ammonia-water hybrid absorption-compression heat pump*) by Jonas Kjaer Jensen, Ph.D. Thesis, Kongens Lyngby December 2015, DTU Mechanical Engineering, Technical University of Denmark.
6. Development of the Hybrid Absorption Heat Pump Process at High Temperature Operation, by Anders Borgås, Masters Thesis June 2014, NTNU Department of Energy and Process Engineering, Norwegian University of Science and Technology.
7. An Introduction to the Kalina Cycle, reprinted by Henry A. Mlcak, PE , first published in PWR- Vol.30, Proceedings of the International Joint Power Generation Conference, with editors: L. Kielasa and G.E. Weed, Book No. H01077-1996.
8. Guide to Water and Sanitation Tariffs used in the City of Cape Town with Level 6 (2017/18) restrictions applicable from 1 February 2018, to Continue Top Service Delivery, published by the City of Cape Town:
<http://www.capetown.gov.za/tariffs>

9. Thermophysical Properties of NH₃ + H₂O solutions for the industrial design of absorption refrigeration equipment, by Dr Manuel R. Conde-Petit (M. Conde Engineering, Zurich - Switzerland) 2004.
10. Evaluation of thermodynamic properties of ammonia-water mixture up to 100 bar for power application systems, by N. Shankar Ganesh and T. Srinivas of the Vellore Institute of Technology, Vellore-632014, India. This paper was published in Journal of Mechanical Engineering Research Vol. 3. (1), pp. 25-39, January, 2011.
11. Analysis of Absorber Operations for the 5 kW Ammonia/Water Combined Cycle by Sirisha Devi Govindaraju as Thesis Presented to the Graduate School of the University of Florida in Partial Fulfillment of the requirements for the Degree of Master of Science, 2005.
12. Thermodynamic Properties of Water including Vapor, Liquid and Solid Phases, by J.H. Keenan, F.G. Keeyes, P.G. Hill, J.G. Moore and published by John Wiley & Sons Inc 1969.
13. Thermodynamic Properties of Ammonia by Lester Haar and John S. Gallager, published in J. Phys. Chem. Ref. Data, Vol. 7, No. 3, 1978.

Publications:

14. Paper presented at PowerGen Africa Conference July 2017 and published in the conference proceedings titled "Introducing a novel thermodynamic cycle (patent pending), for the economic power generation from recovered heat pumped from the huge global thermal energy reservoir called earth" by Johan Enslin, Heat Recovery Micro System CC. This paper is also accessible from my website http://www.heatrecovery.co.za/.cm4all/iproc.php/PowerGen-Africa 2017 Proceedings Speaker0 Session19149_1.pdf
15. A Paper titled "The Simplified REHOS Cycle.pdf" was written by Johan Enslin in August 2017 and published on my website <http://www.heatrecovery.co.za/.cm4all/iproc.php/The Simplified REHOS Cycle.pdf>
16. A Paper titled "Clarifying Process Parameters for the REHOS Cycle Concept_rev3.pdf" was written by Johan Enslin in October 2017 and published on my website http://www.heatrecovery.co.za/.cm4all/iproc.php/Clarifying Process Parameters for the REHOS Cycle Concept_rev3.pdf
17. The Paper titled "The Binary NH₃-H₂O Bubble Reactor_rev1.pdf" was written by Johan Enslin in December 2017, but as yet unpublished. Should you need this document, contact myself at: <mailto:johan.enslin@heatrecovery.co.za>

18. The Paper titled "The Competitive Advantages of REHOS Technology_rev1.pdf" was compiled by Johan Enslin in early January 2018, and published on my website [http://www.heatrecovery.co.za/cm4all/iproc.php/Competitive Advantages of REHOS Technology_rev1.pdf](http://www.heatrecovery.co.za/cm4all/iproc.php/Competitive%20Advantages%20of%20REHOS%20Technology_rev1.pdf)
19. Another paper, "Executive Overview of the REHOS Technology_rev1.pdf" was compiled by Johan Enslin in February 2018 and published on my website [http://www.heatrecovery.co.za/cm4all/iproc.php/Executive Overview of the REHOS Technology_rev1.pdf](http://www.heatrecovery.co.za/cm4all/iproc.php/Executive%20Overview%20of%20the%20REHOS%20Technology_rev1.pdf)
20. The follow-up document "Clarification of COP calculations for Absorption Heat Transformer (AHT) Type Heat Pumps.pdf" was written by Johan Enslin (to enhance the Executive Overview paper) in March 2018 and published on my website [http://www.heatrecovery.co.za/cm4all/iproc.php/Clarification of COP calculations for Absorption Heat Transformer \(AHT\) Type Heat Pumps.pdf](http://www.heatrecovery.co.za/cm4all/iproc.php/Clarification%20of%20COP%20calculations%20for%20Absorption%20Heat%20Transformer%20(AHT)%20Type%20Heat%20Pumps.pdf)
21. The document titled "Comparison of various Modern Heatpump Technologies for unlocking Commercial Value from Ambient Heat_rev4.pdf" was written by Johan Enslin in April 2018 and published on my website [http://www.heatrecovery.co.za/cm4all/iproc.php/Comparison of various Modern Heatpump Technologies for unlocking Commercial Value from Ambient Heat_rev4.pdf](http://www.heatrecovery.co.za/cm4all/iproc.php/Comparison%20of%20various%20Modern%20Heatpump%20Technologies%20for%20unlocking%20Commercial%20Value%20from%20Ambient%20Heat_rev4.pdf)
22. Website for Heat Recovery Micro Systems where the above publications are available from: www.heatrecovery.co.za

Appendix A:

Table 4

Process Parameters at Design Point

Description	Position	Line ID m	Line Size	Flow Area m ²
Bubble Reactor Top Liquid Level	A	2.647E-01	10"	5.502E-02
Bubble Reactor Bottom Liquid Level	B	2.647E-01	10"	5.502E-02
Pump Inlet Liquid Line	C	8.000E-03	10mm	5.027E-05
HP Pump Outlet Liquid Line	D	8.000E-03	10mm	5.027E-05
Evaporator Heat Exchanger Liquid Entry	E	8.000E-03	10mm	5.027E-05
Evaporator Heat Exchanger Vapor Exit	F	8.000E-03	10mm	5.027E-05
HP Vapor from Evaporator	G	8.000E-03	10mm	5.027E-05
Start-up HP Recirc Mixture	H	8.000E-03	10mm	5.027E-05
Start-up LP Recirc Mixture	I	8.000E-03	10mm	5.027E-05
Ejector Jet Drive Vapor	J	8.000E-03	10mm	5.027E-05
Suction Vapor Line	K	1.580E-02	1/2"	1.961E-04
Suction Vapor Ejector Inlet	L	4.000E-02	40mm	1.257E-03
Ejector Outlet Line	M	2.664E-02	1"	5.574E-04
Bubble Vapor Plenum	N	2.647E-01	10"	5.502E-02
Suction Vapor Plenum	O	2.647E-01	10"	5.502E-02

Table 5

Process Parameters at Design Point

Position	Mass Flow kg/s	Density kg/m ³	%NH ₃	Flow Speed m/s	Pressure Pa Abs	Temp Celsius
A	N/A	665	100.0%		1.927E+05	-20
B	N/A	911	6.0%		2.001E+05	100
C	1.270E-03	665	100.0%	0.038	1.927E+05	-20
D	1.270E-03	665	100.0%	0.038	6.234E+05	-20
E	1.270E-03	665	100.0%	0.038	6.234E+05	-20
F	1.270E-03	4.9	100.0%	5.19	6.234E+05	10
G	1.270E-03	4.9	100.0%	5.19	6.234E+05	10
H	0.000E+00	4.9	100.0%	0.00	6.234E+05	10
I	0.000E+00	1.6	100.0%	0.00	2.001E+05	10
J	1.270E-03	4.9	100.0%	5.19	6.234E+05	10
K	5.459E-03	1.6	100.0%	17.36	1.927E+05	-20
L	5.459E-03	1.6	100.0%	2.71	1.927E+05	-20
M	6.729E-03	1.8	100.0%	6.65	2.198E+05	-17
N	6.729E-03	1.7	100.0%	0.074	2.004E+05	-17
O	5.459E-03	1.6	100.0%	0.062	1.927E+05	-20

Table 6

Process Parameters at Design Point

Position	Quality X	2PH Density kg/m ³	Q _{vap} m ³ /s	Q _{liq} m ³ /s	Void
A	0.241%	333	3.403E-03	2.7567E-02	11.0%
B	0.181%	456	4.065E-03	2.7551E-02	12.9%

Table 7**Process Parameters at Design Point**

Position	Mass Flow kg/s	Density kg/m³	Temp Celsius	Pressure Pa Abs	Enthalpy J/kg	Liq/Vap
A	N/A	665	-20	1.927E+05	-9.133E+04	Liq
B	N/A	911	100	2.001E+05	3.777E+05	Liq
C	1.270E-03	665	-20	1.927E+05	-9.133E+04	Liq
D	1.270E-03	665	-20	6.234E+05	-9.133E+04	Liq
E	1.270E-03	665	-20	6.234E+05	-9.133E+04	Liq
F	1.270E-03	4.9	10	6.234E+05	1.272E+06	Vap
G	1.270E-03	4.9	10	6.234E+05	1.272E+06	Vap
H	0.000E+00	4.9	10	6.234E+05	1.272E+06	Vap
I	0.000E+00	1.6	10	2.001E+05		Vap
J	1.270E-03	4.9	10	6.234E+05	1.272E+06	Vap
K	5.459E-03	1.6	-20	1.927E+05	1.238E+06	Vap
L	5.459E-03	1.6	-20	1.927E+05	1.238E+06	Vap
M	6.729E-03	1.8	-17	2.198E+05	1.207E+06	Vap
N	6.729E-03	1.7	-17	2.004E+05	1.242E+06	Vap
O	5.459E-03	1.6	-20	1.927E+05	1.238E+06	Vap